Representation, Characterization and Simulation of Tool-Part Interaction and its Effects on Process-induced Deformations in Composites

Caleb Schoenholz; Daniel Slade; Enrico Zappino; Marco Petrolo; Navid Zobeiry

OFFICIAL CONFERENCE PUBLICATION

Proceedings of the American Society for Composites - Thirty-Sixth Technical Conference on Composite Materials (2021)

https://doi.org/10.12783/asc36/35832

RELATED SUBSTANTIALLY EXTENDED JOURNAL ARTICLE

C. Schoenholz and N. Zobeiry, "Investigating the Impacts of Processing Variability on Tool-Part Interaction for Interply-Toughened Aerospace Composites Using a Novel Shear Technique," Composites Part A 178, 107973 (2024).

https://doi.org/10.1016/j.compositesa.2023.107973

ABSTRACT

The interaction between a tool and part during composites processing contributes to the formation of residual stresses and dimensional changes. A resultant mismatch of part geometries during assembly can cause a potential loss of mechanical performance in aerospace structures. Costly shimming steps are needed to compensate for process-induced deformations and satisfy specifications on mechanical performance. Due to difficulties associated with accurate measurement of interfacial shear stresses, current analysis methods fail to represent the interaction between a tool and part throughout processing. A combined approach to represent, characterize, and simulate tool-part interaction and its effects on dimensional changes is proposed. First, a characterization method was established using a custom Dynamic Mechanical Analysis (DMA) shear test setup to measure tool-part interfacial stress development in a simulated autoclave curing environment. Tool-part interfacial stresses were characterized for Toray T800S/3900-2 UD prepreg as a function of temperature, degree of cure, strain rate, and tool surface condition. Then, a previously developed numerical model was modified to include the effects of tool-part interaction in predicting dimensional changes of L-shape parts. For validation, composite parts were fabricated on tools with different surface conditions and successfully compared to simulation results. This paper demonstrates that tool-part interaction significantly impacts the spring-in of angled composite parts. The proposed method is a comprehensive and practical approach to study and simulate the effects of tool-part interaction. The results of this paper can be used to understand the complex interaction between a tool and part throughout processing and potentially mitigate process-induced deformations.

Caleb Schoenholz[1], Daniel Slade[1], Enrico Zappino[2], Marco Petrolo[2], Navid Zobeiry[1,*]

[1]Materials Science & Engineering Department, University of Washington, Seattle, WA 98195, USA

[2]MUL2 Group, Department of Mechanical and Aerospace Engineering, Politecnico di Torino, Corso Duca degli Abruzzi 24, 10129 Torino, Italy

*Corresponding author, (206) 221-3254, navidz@uw.edu

1. INTRODUCTION

Many factors contribute to formation of residual stresses during processing of composite parts and consequently process-induced deformations (PIDs) [1,2]. Mismatch of free strains (i.e., cure shrinkage and thermal strains) at different scales of micro-, macro-, coupon-, and component-levels is a major contributing factor to PIDs [3]. Other factors, however, may significantly contribute to PIDs including the degree of tool-part interaction [3-9] in the form of weak bonds and/or interfacial friction.

Typically for a composite part, two types of PIDs are considered as schematically shown in Fig. 1: warpage of parts cured on flat tools, and spring-in of parts cured on curved tools [1-12]. While the warpage of flat parts is developed due to the mismatch of tool and part free strains (e.g., CTE) and the degree of tool-part interaction, the spring-in is typically associated with the orthotropy of free strains in composites (i.e., through-thickness versus in-plane strains) as well as tool-part interaction [10]. Due to tool-part interaction, a through-thickness shear stress distribution is developed and locked in the part as curing progresses. Some of this internal residual stress is released via bending deformation upon demolding, which in turn results in part warpage and spring-in (Fig. 1a and b, respectively). The magnitude of warpage is directly related to the level of tool-part interaction [12].

Both warpage and spring-in can cause significant performance-related problems during the assembly of aerospace structures. Techniques such as shimming are commonly used to compensate for PIDs and meet tolerance requirements for assembly of aerospace components. However, such methods are time consuming, costly, and can potentially reduce mechanical performance [10]. A more robust approach is to take advantage of process simulation to mitigate PIDs using tool geometry compensation and optimization of process parameters. An effective process simulation approach, however, requires robust material characterization techniques including methods to accurately quantify the degree of tool-part interaction.

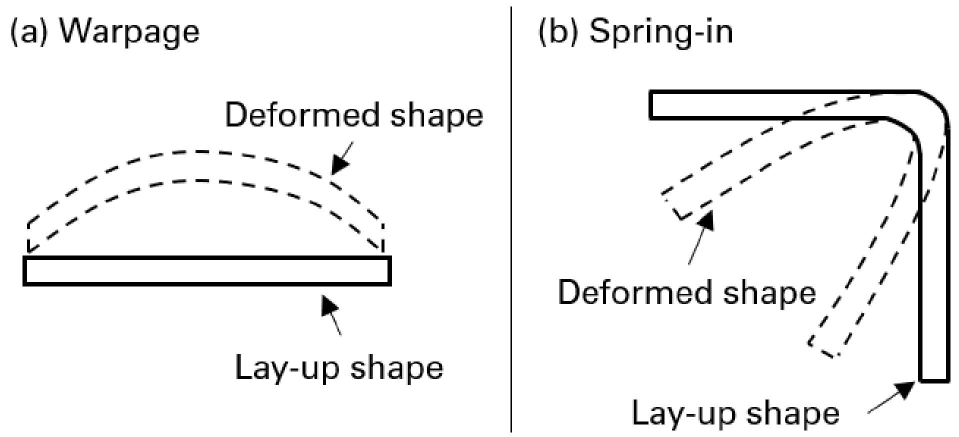

Fig. 1 (a) Warpage of flat parts (b) spring-in of curved parts.

Several previous studies have focused on characterizing tool-part interaction [6,7,12]. Albert and Fernlund [12] examined the effects of several design and process parameters on PIDs of angled composite parts. Tool surface condition was shown to substantially affect the overall spring-in and warpage of L-shape parts. Parts processed on a tool covered with a Frekote release agent showed considerably greater spring-in and warpage than those processed on a tool covered with a sheet of fluorinated ethylene propylene (FEP) and release agent. Measuring PIDs was shown to be a qualitative way of assessing the level of tool-part interaction that occurred during processing.

Twigg et al. [6] quantified tool-part interaction effects by curing composite parts in an autoclave using a thin aluminum tool instrumented with strain gauges. The authors found that the CTE mismatches between tool and part create three separate interfacial shear stress regimes. The first interfacial regime is sticking, where the tool and part develop an adhesive bond. Next is debonding, where the tool-part adhesive bond breaks with a sharp drop in the interfacial shear stress. After debonding, a sliding regime is developed, where shear stress remains constant based on kinetic friction forces. Experimentally, measuring the magnitudes of debonding and sliding stresses was shown to sufficiently quantify the level of tool-part interaction throughout processing.

Ersoy et al. [7] measured prepreg/prepreg and tool/prepreg interfacial stresses in a simulated autoclave curing environment. The authors mounted an apparatus in a standard tensile testing machine where an aluminum strip was sandwiched between two composite strips and pulled out at a controlled rate. The real-time force required for pull-out was recorded throughout the cure cycle and used to calculate interfacial shear stresses. The authors verified Twigg et al.'s findings on sticking, debonding, and sliding stress regimes. Additionally, their results showed that tool-part adhesive bonding occurred only when the tool surface was covered with a release agent. FEP film was shown to prevent adhesive bonding and lowered the magnitudes of interfacial stresses. The effects of FEP were also highlighted by Twigg et al. [6], and can be additionally supported by the experimental results of Albert and Fernlund [12].

This paper presents a novel calibration technique to directly measure tool-part interfacial shear stress development using a custom-built shear test fixture in a DMA. The experimental setup allows for quick measurement of interfacial stresses as a function of many contributing factors including temperature, lay-up, degree of cure, strain rate, compaction level, and tool surface condition. For validation, characterized properties are used to predict spring-in angle in L-shape parts fabricated on different tool surface conditions.

2. CHARACTERIZING TOOL-PART INTERACTION

2.1 Sample Preparation

Composite samples used for measuring tool-part interaction in this study were made using a UD carbon/epoxy prepreg system by Toray Industries, Inc. with the designation of T800S/3900-2. To prepare each sample, ten plies with nominal dimensions of 5 mm × 5 mm were cut using an X-ACTO® knife. The plies were then stacked to create two cross-ply laminates with $[0/90/\bar{0}]_s$ layups. Both laminates were simultaneously hot-debulked for 30 minutes at 140°C on a hotplate under approximately 0.7 MPa of applied pressure from caul plates. The laminates were cooled down to room temperature before testing in the DMA.

2.2 Apparatus

A custom testing setup was constructed using the shear sandwich clamp in the TA Instruments® Discovery Dynamic Mechanical Analyzer (DMA) 850. First, the moveable and stationary clamp faces were covered with one and three layers of silicone adhesive tape, respectively. Next, custom U- and C-shape steel tools were positioned over the moveable and stationary clamps. The composite laminates were then sandwiched between the tools with the 0° plies facing upwards. A torque-limiting screwdriver was used on the fixture's knurled knobs to apply 0.7 MPa of pressure on the laminates. Fig. 2 shows an image of the custom DMA shear test setup.

SOFT SILICONE LAYERS

During processing, cross-ply composite laminates may shrink by about 1% in the through-thickness direction [13]. This is partly due to cure shrinkage, partly due to thermal shrinkage during cool-down, and partly due to Poisson's effects of in-plane strains. Soft silicone layers were placed in the system to mitigate shrinkage-induced pressure loss by counteractively expanding in the through-thickness direction during heat-up. Without thermally-expanding layers, the shrinkage of the composite parts would cause a loss of pressure in the DMA test setup. Soft layers were placed underneath the U- and C-shape tools to ensure the pressure remained at or above 0.7 MPa throughout the test. The thickness and total number of layers were estimated based on the thermal expansion properties of silicone during heat-up. The pressure amount was measured before and after each test to verify the effect of soft layers.

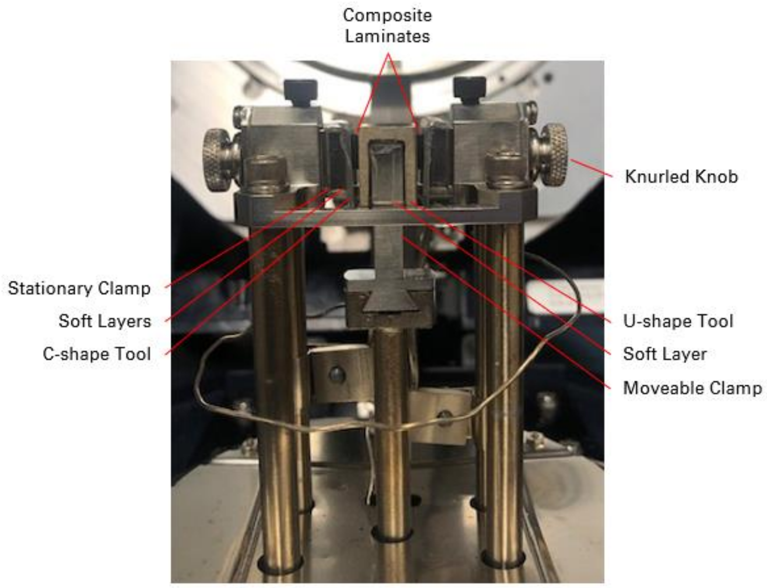

Fig. 2. Custom DMA shear test setup for characterizing tool-part interaction. Composite laminates are sandwiched between U- and C- shape tools. Laminates remain strongly bonded to abraded C-shape tools and form weaker bonds with U-shape tool covered with release agent or FEP.

U-SHAPE TOOL

A custom U-shape tool made of A2 tool steel was machined with an inner-gap width of 5.6 mm and outside-surface dimensions of 12.7 mm × 12.7 mm to ensure a secure fit in the testing apparatus. The U-shape configuration of the tool is necessary to prohibit unwanted motion in the vertical direction during testing. Before each test, the tool surfaces were cleaned with acetone to eliminate any residue from previous tests. The surfaces were then treated with three layers of Henkel LOCTITE® FREKOTE 710-NC™ release agent or covered with one layer of FEP film depending on the test procedure. The release agent was applied with a brush following the Data Sheet directions.

C-SHAPE TOOLS

Before each test, two disposable C-shape tools made of A2 tool sheet steel were prepared using a manual shear/brake combination machine. Each C-shape had top and bottom horizontal-side lengths of 5 mm and 10 mm, respectively, and a vertical-side length of 15 mm. The tools had a uniform width of 12.7 mm. The C-shape configurations are necessary to restrict unwanted vertical motion during testing. The outside surfaces of the C-shapes were roughened using 80 grit aluminum oxide sandpaper for two minutes. The abraded surfaces were then cleaned with isopropyl alcohol (IPA) to remove any steel dust created during sanding. The C-shapes were disposed of after each test.

2.3 Test Procedure

The following test procedures were used to experimentally characterize tool-part debonding and sliding stresses for release agent- and FEP-prepared tool surface conditions. Capturing the interfacial debonding and sliding regimes required different test methods. It was only necessary to perform a sliding stress test for the FEP surface condition since the use of FEP prevents any degree of tool-part bonding.

DEBONDING TEST

Once the composite samples were loaded into the DMA shear sandwich setup, the system was subjected to a temperature cycle following the Manufacturer's Recommended Cure Cycle (MRCC). The MRCC consists of a temperature ramp from 30°C to 180°C at 2°C/min and hold at 180°C for 120 minutes, with 0.7 MPa of pressure applied throughout processing. The cool-down portion of the MRCC was not performed in this study. During heat-up, the laminates begin to cure, and the outwards-facing plies form strong primary bonds as well as mechanical bonds with the abraded C-shape tool surfaces. The composites remain bonded and fixed to the stationary C-shapes throughout the test. The inwards-facing plies of the laminates form weaker primary and secondary bonds with the U-shape tool since its surfaces are covered with release agent or FEP. The laminates are held stationary during cure until their gel points where tool-part stresses start to evolve [6,7]. The gelation was estimated to occur 85 minutes into the cure cycle using bi-material beam tests conducted with DMA [1].

Upon gelation, an upwards force was applied from the DMA drive motor to create vertical motion in the U-shape tool. This created a constant strain rate which was applied through the remaining time of the cure cycle. The composite samples remained stationary as they were strongly bonded to the outside C-shapes. The relative movement between the U-shape tool and composites simulated a tool-part shear interaction during processing due to CTE mismatches. Three displacement rates of 0.001, 0.003 and 0.01 mm/min were chosen for the tests. In all experiments, tool-part debonding occurred between 0.2-0.5 mm of applied displacement. The 0.001 mm/min strain rate was not fast enough to cause tool-part debonding within the timeframe of the cure cycle. Therefore, the results obtained from the 0.001 mm/min strain rate are not discussed further in this paper. A duplicate test was conducted using the 0.003 mm/min strain rate and demonstrated consistent results.

The DMA recorded forces to produce the shear strain throughout the cure cycle. The forces were then divided by the effective sample area to calculate tool-part interfacial shear stresses. The maximum stress value before a sharp drop was considered the tool-part debonding stress.

SLIDING TEST

After the debonding test procedure was complete for the release agent surface condition, the system's pressure was readjusted to 0.7 MPa using the torque-limiting screwdriver and knurled knobs. The temperature was then equilibrated, and a strain ramp was applied through the U-shape tool until the recorded force values plateaued. The magnitude of sliding forces is equivalent to kinetic friction, which depends on several factors including material properties of the two contacting objects and the normal force pushing them together. A 0.1 mm/min strain rate was chosen for the sliding stress tests to achieve force plateaus in a minimal amount of time. Sliding stresses were measured for release agent and FEP surface conditions at 180°C. Since there was no debonding procedure for the FEP condition, sliding was characterized using previously cured composite samples. Tool-part interfacial stress and strain were calculated using the same method as in the debonding stress tests. The average stress value in the plateau region was considered the tool-part sliding stress.

3. TOOL-PART INTERACTION TEST RESULTS AND DISCUSSION

3.1 Debonding

Fig. 3 shows interfacial stress τ versus time for two tests with different shear strain rates of 0.003 and 0.01 mm/min. The respective strain rates are denoted by subscripts in the plot's legend. The units of the strain rates are omitted from the remainder of this section for simplification purposes. The temperature profile and simulated degree of cure are also shown in the graph. Tool-part stresses were confined at zero until the strain rates were applied at the gel point. The two strain rates resulted in similar interfacial stress trends. Both curves exhibit a gradual increase in slope to linear behavior, sharply drop to a lower value, then either continue to rise or plateau through the end of the cycle.

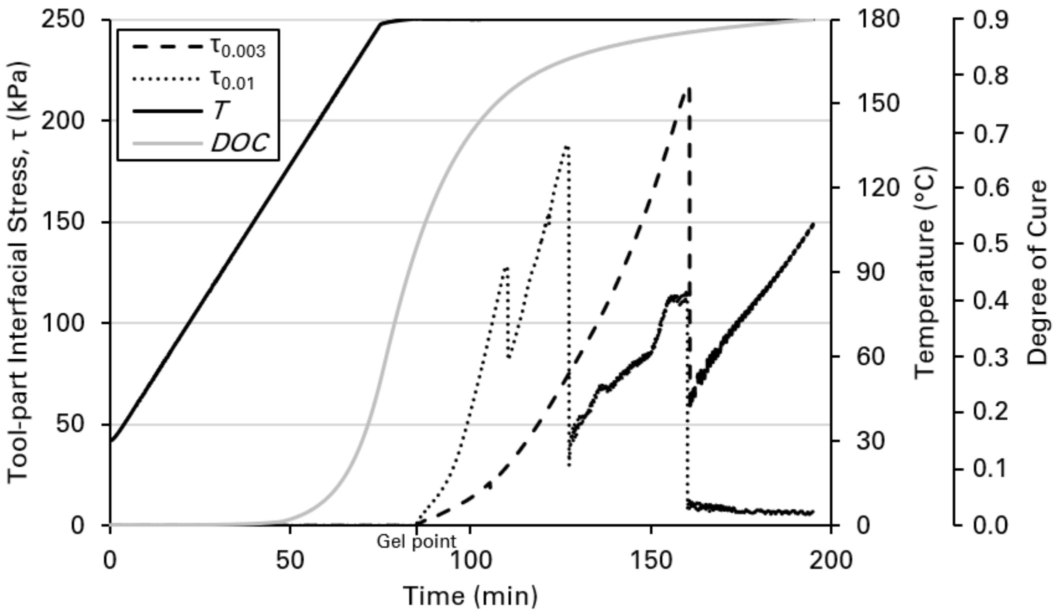

Fig. 3. Temperature (T), degree of cure (DOC), and tool-part interfacial shear stress (τ) versus time for release agent tool surface condition using 0.003 and 0.01 mm/min strain rates.

The initial rise in magnitude seen in both stress curves represents tool-part sticking behavior. Both curves exhibit a gradual increase in slope rather than being entirely linear from the start. The non-linearity in the early stages of the curves suggests the tool-part bond stiffness is increasing during this time. This behavior is especially apparent in the test results from the slower 0.003 strain rate. The curve from the faster 0.01 rate shows non-linear behavior only for a brief period. This can be explained based on the evolution of degree of cure and consequent increase of the resin's shear modulus.

The interfacial stress progresses to a maximum value then sharply drops. The maximum stress value before the sharp drop is considered the tool-part debonding stress. The debonding stress is equivalent to the ultimate strength of the tool-part bond for the given temperature and degree of cure. Fig. 4 shows interfacial stress versus strain for the tests with different strain rates reported in Fig 3. The 0.01 stress curve exhibits an intermediate sharp drop before rising to its maximum value. This may be due to slippage between laminate plies or partial debonding of tool and part. The tool-part debonding stresses for the two strain rates, $\tau_{db,0.003}$ and $\tau_{db,0.01}$, were 220 and 190 kPa, respectively. These results suggest the magnitude of debonding may be affected by strain rate. This is consistent with previous results in the literature [7]. The slope of the curve was much steeper in the 0.003 test immediately before debonding, which suggests the tool-part bond stiffness was greater at failure for the slower rate. This higher stiffness could be because tool-part debonding occurred later in the cure cycle for the slower strain rate, so the composite sample progressed to a higher degree of cure and was able to form stronger bonds with the tool.

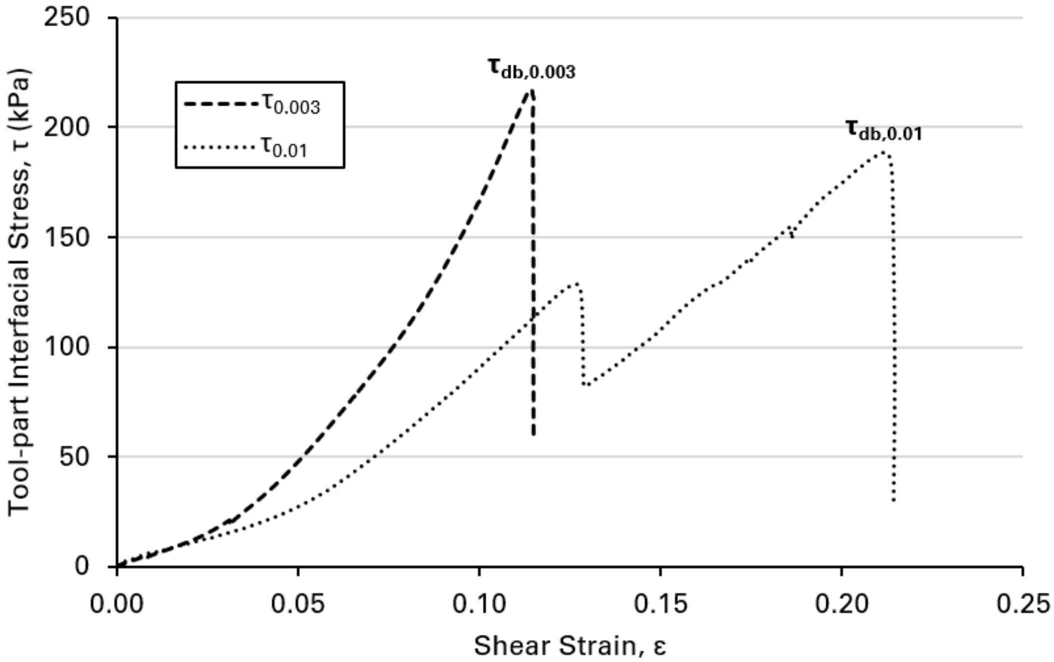

Fig. 4. Tool-part interfacial shear stress (τ) versus strain (ε) at 180°C for release agent tool surface condition with 0.003 and 0.01 mm/min strain rates until tool-part debonding stress (τ_{db}).

The post-debonding stress regimes in Fig. 3 show non-idealized behavior that differs from previous reports. Once a tool and part debond, the interfacial stress magnitude should follow kinetic friction forces only. Both stress curves in Fig. 3 show rises in stress after debonding. The additional increases in stress may be due to subsequent tool-part sticking at high temperatures.

3.2 Sliding

Fig. 5 shows tool-part interfacial stress τ versus strain ε for release agent (RA) and FEP tool surface conditions at 180°C. The respective tool surface conditions are denoted by subscripts in the plot's legend. The average stress value for each surface condition was considered the tool-part sliding stress. The tool-part sliding stresses for the RA and FEP surface conditions were 160 and 120 kPa, respectively. The FEP sliding stress magnitude can be considered the maximum tool-part stress developed throughout the cycle as no sticking or debonding behaviors occur. The tool-part stress with the FEP surface condition was notably lower than the release agent sliding value of 160 kPa. The maximum FEP stress value of 120 kPa was also significantly lower than the release agent debonding stresses of 190 and 220 kPa. A substantial reduction in maximum interfacial stress suggests the use of FEP film reduces the level of tool-part interaction. Similar trends have been reported in previous studies and are explained by FEP film's impermeable properties [6,7,12]. FEP acts as a barrier to prevent any tool-part bonds and adhesion during the cure cycle. On the other hand, release agent does not entirely restrict tool-part adhesion but rather limits it through secondary bonding mechanisms.

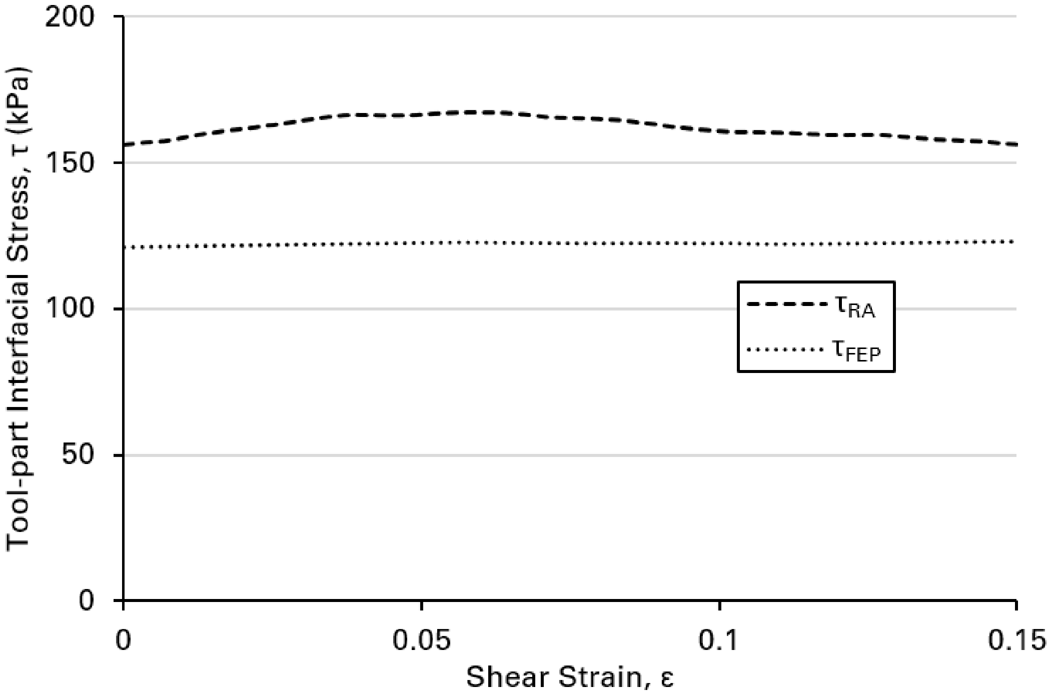

Fig. 5. Tool-part interfacial shear sliding stress (τ) versus strain (ε) at 180°C for release agent (RA) and FEP tool surface conditions.

4. VALIDATION TESTS AND SIMULATION

An effective process simulation approach requires robust characterization of material properties such as shear modulus and free strains. However, these properties have not been previously characterized or reported in the literature for Toray T800S/3900-2. Therefore, validation tests and simulations were conducted using the previously characterized HEXCEL AS4/8552 [8]. It was assumed that the degree of tool-part interaction during processing of T800S/3900-2 and AS4/8552 parts would follow similar trends for RA and FEP surface conditions. The trends in simulation results using AS4/8552 properties would therefore be valid for the T800S/3900-2 material system.

First, several L-shape laminates made from AS4/8552 with $[0]_8$ layups were fabricated on a steel tool with two different surface conditions: three layers of Frekote release agent and FEP. For each surface condition, three specimens were fabricated using a one-hold temperature cycle at 180°C, following the MRCC. Each specimen had a width of 50 mm and a flange length of 100 mm. The L-shape samples fabricated on the tool prepared with release agent had an average of 1.11° corner spring-in angle and 0.09° of flange warpage. The samples fabricated on the FEP-prepared tool had only 1.06° of spring-in angle and 0.02° of flange warpage. Here we present simulation results for fabrication of L-shape parts on tools with different surface conditions.

4.1 Numerical Model

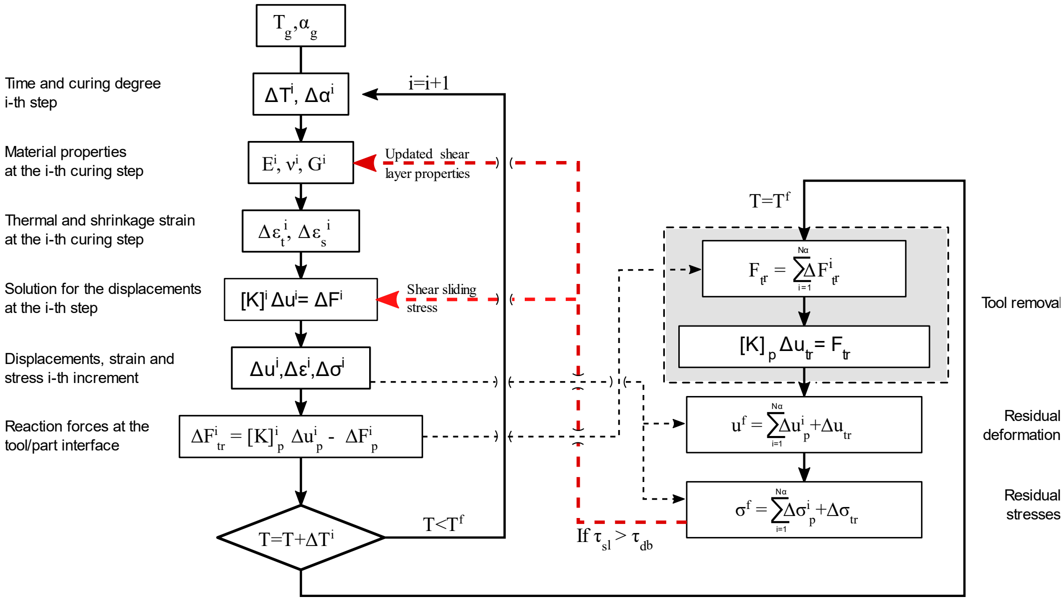

Fig. 6. Numerical solution scheme; in red the implementation of the tool-part interaction.

A refined numerical model was used to predict the tool-part interaction effects on process-induced deformations. The numerical approach, previously presented by Zappino et al. [8], is based on a refined kinematic model developed in the framework of the Carrera Unified Formulation (CUF). A layer-wise approach was used to accurately describe displacement and stress fields at the lamina level. The interface between the tool and the part was modelled through a shear layer. The properties of the shear layer were assumed equal to those of the resin, and the debonding and sliding stresses were taken from the experimental tests presented before. The thickness of the shear layer was set to one-tenth of a single lamina.

Three tool-part interfaces were considered. First, no interactions were accounted for; then, the FEP layers and the use of release agent (RA) were considered. The iterative solution scheme used in the numerical analysis is presented in Fig. 6. At each time step, a debonding check was carried out. When the shear stress in the shear layer, τ_{sl}, becomes higher than the debonding stress, τ_{db}, the stiffness of the shear layer is reduced to simulate the debonding and, in the case of RA, sliding stress is applied. More details on the solution approach can be found in [8].

4.2 Numerical Results

Fig. 7 shows the spring-in angle and flange warpage for the three cases considered. Experimental and numerical results are compared. Without tool-part interaction, the spring-in angle is 0.79°, with a warping of 0.03°. The introduction of the FEP layers slightly increases the spring-in angle to 0.825°. The introduction of tool-part interaction due to the FEP layers has a more significant effect on the warping that increases by 50%, assuming a value of 0.045°. The use of the release agent further increases the spring-in angle to 0.87°, with a warping of 0.07°.

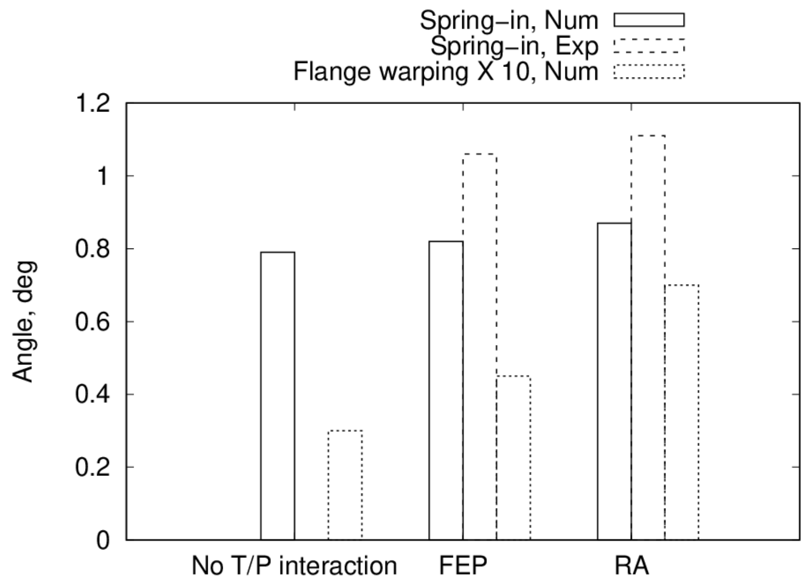

Fig. 7. Spring-in angle and flange warping for the three cases considered.

Experimental and numerical results for PIDs in L-shape parts are compared in Table I. The values of the spring-in angle are comparable with those from the experimental results, even if the numerical model underestimates the spring-in angle by 20%. The general trend of the results confirms the effectiveness of the interface modelling. The numerical model predicts an increment in the spring-in angle of 5.4% when the release agent is used compared to the FEP case. The value is confirmed by the experimental results that show an increment of 4.7%. The discrepancies in the absolute value of the spring-in angle may be due to the curing model of the material at the early stage after the gelation point. Inaccurate moduli, especially in the shear evolution, can create significant differences in the residual deformations.

Fig. 8 shows the time evolution of the debonding for the FEP and RA models. The darkest areas are those where the debonding happens first. It can be seen that when FEP layers are used, the debonding takes place starting from minute 70 to minute 81, while the use of the RA postpones the debonding from minute 75 to minute 86. In both cases, the debonding appears first in the transition area between the corner and the flange. The use of layers of FEP makes the debonding more uniform on the flange, thus, reducing the final warping.

TABLE I. SUMMARY OF EXPERIMENTAL AND NUMERICAL RESULTS FOR PIDs OF L-SHAPE PARTS

Surface Condition	Tool-Part Interaction		Experimental PIDs		Numerical PIDs	
	Debonding Stress	Sliding Stress	Spring-in	Warpage	Spring-in	Warpage
Release Agent	190-220 kPa	160 kPa	1.11°	0.09°	0.87°	0.07°
FEP	120 kPa		1.06°	0.02°	0.82°	0.04°

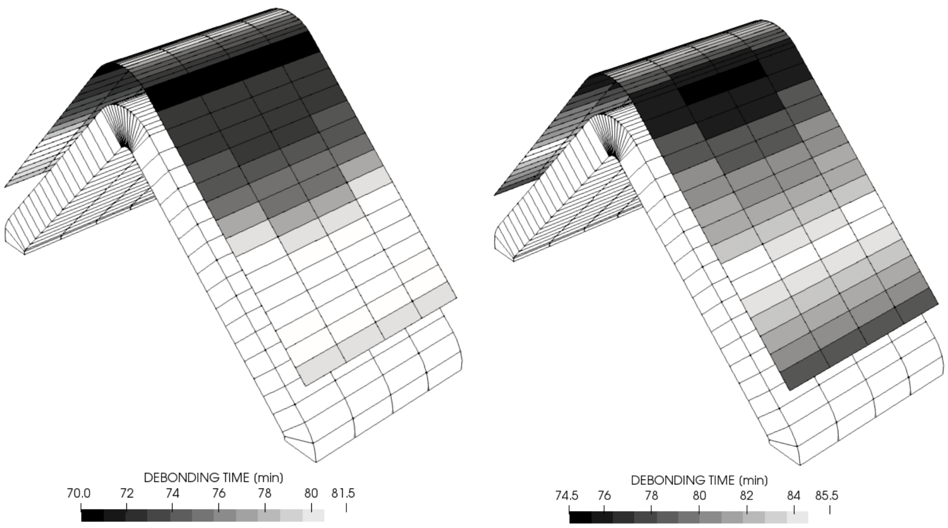

Fig. 8. Debonding time evolution for the FEP interface (left) and RA (right).

5. CONCLUSION

The first objective of this study was to develop a quick experimental technique to directly characterize tool-part interaction during composites processing. A custom DMA shear test setup was used to measure tool-part interfacial stresses for Toray T800S/3900-2 as a function of tool surface condition. The experimental results were then implemented into a refined kinematic model to predict the effects of tool-part interaction on process-induced deformations. The main conclusions from this work are as follows:

- During processing, a tool covered in release agent shows three interfacial stress regimes of tool-part interaction: sticking, debonding, and sliding. When a tool is covered in FEP, tool and part only exhibit sliding behavior that is dependent on kinetic friction forces. The use of FEP film lowers the magnitude of tool-part interfacial stresses.
- The magnitude of tool-part debonding stress potentially depends on degree of cure and strain rate.
- The spring-in and warpage of L-shape parts showed to be affected by tool-part interaction. L-shape parts fabricated on tools covered in FEP showed less spring-in and warpage than parts fabricated on tools covered in three layers of release agent.
- The present kinematic model can predict the general trends of PIDs due to tool-part interaction. For L-shape parts, trends of both spring-in angle and warping variations matched the experimental results. The numerical model was also used to predict spatial and temporal propagation of the tool-part debonding during processing.

ACKNOWLEDGEMENTS

The work reported here was funded by Toray Industries, Inc. The authors would like to specifically acknowledge Toshiya Kamae, Benjamin Rutz, and Dongyeon Lee for their insight regarding composites processing.

REFERENCES

1. Zobeiry, N., A. Forghani, C. Li, K. Gordnian, R. Thorpe, R. Vaziri, G. Fernlund, A. Poursartip. 2016. "Multiscale characterization and representation of composite materials during processing," *Phil. Trans. R. Soc. A*, 374: 20150278.
2. Li, C., N. Zobeiry, S. Chatterjee, and A. Poursartip. 2014. "Advances in the characterization of residual stress in composite structures," in *SAMPE Conf., Society for the Advancement of Material and Process Engineering*, Seattle, WA.
3. Twigg, G., A. Poursartip, and G. Fernlund. 2004. "Tool–part interaction in composites processing. Part I: experimental investigation and analytical model," *Composites Part A: Applied Science and Manufacturing*, 35(1): 121-133.
4. Twigg, G., A. Poursartip, and G. Fernlund. 2004. "Tool–part interaction in composites processing. Part II: numerical modelling," *Composites Part A: Applied Science and Manufacturing*, 35(1): 135-141.
5. Potter, K. D., M. Campbell, C. Langer, and M. R. Wisnom. 2005. "The generation of geometrical deformations due to tool/part interaction in the manufacture of composite components," *Composites Part A: Applied Science and Manufacturing*, 36(2): 301-308.
6. Twigg, G., A. Poursartip, and G. Fernlund. 2003. "An experimental method for quantifying tool–part shear interaction during composites processing," *Composites Science and Technology*, 63(13): 1985-2002.
7. Ersoy, N., K. Potter, M. R. Wisnom, and M. J. Clegg. 2005. "An experimental method to study the frictional processes during composites manufacturing," *Composites Part A: Applied Science and Manufacturing*, 36(11): 1536-1544.
8. Zappino, E., N. Zobeiry, M. Petrolo, R. Vaziri, E. Carrera, and A. Poursartip. 2020. "Analysis of process-induced deformations and residual stresses in curved composite parts considering transverse shear stress and thickness stretching," *Composite Structures*, 241: 112057.
9. Fernlund G., C. Mobuchon, and N. Zobeiry. 2018. "2.3 Autoclave Processing," in *Comprehensive Composite Materials II*, P.W.R. Beaumont and C.H. Zweben, eds. Oxford: Academic Press, pp. 42-62.
10. Zobeiry N. and A. Poursartip. 2015. "The origins of residual stress and its evaluation in composite materials," in *Structural Integrity and Durability of Advanced Composites*, P.W.R. Beaumont, S. Soutis, and A. Hodzic, eds. Woodhead Publishing, pp. 43-72.
11. Kaushik, V. and J. Raghavan. 2010. "Experimental study of tool–part interaction during autoclave processing of thermoset polymer composite structures," *Composites Part A: Applied Science and Manufacturing*, 41(9): 1210–1218.
12. Albert, C. and G. Fernlund. 2002. "Spring-in and warpage of angled composite laminates," *Composites Science and Technology*, 62(14): 1895–1912.
13. Ersoy, N. and M. Tugutlu. 2010. "Cure kinetics modeling and cure shrinkage behavior of a thermosetting composite," *Polymer Engineering & Science*, 50(1): 84–92.